




Honors Theses at the University of Iowa

Spring 2020

Discovery and Analysis of New Cocrystal Solid Forms of the Anti-HIV Drug: Emtricitabine

Elizabeth Keene

Follow this and additional works at: https://ir.uiowa.edu/honors_theses

 Part of the [Organic Chemicals Commons](#), and the [Pharmaceutical Preparations Commons](#)

This honors thesis is available at Iowa Research Online: https://ir.uiowa.edu/honors_theses/337

DISCOVERY AND ANALYSIS OF NEW COCRYSTAL SOLID FORMS OF THE ANTI-HIV DRUG:
EMTRICITABINE

by

Elizabeth Keene

A thesis submitted in partial fulfillment of the requirements
for graduation with Honors in the Chemistry

Leonard R MacGillivray, Gonzalo Campillo-Alvarado
Thesis Mentor

Spring 2020

All requirements for graduation with Honors in the
Chemistry have been completed.

Claudio J Margulis
Chemistry Honors Advisor

Discovery and Analysis of New Cocrystal Solid Forms of the Anti-HIV Drug: Emtricitabine

by

Elizabeth A. Keene

A thesis submitted in partial fulfillment
of the requirements for graduation with
Honors in Chemistry College of Liberal Arts and Sciences of
the University of Iowa

May 2021

Prof. Leonard R. MacGillivray, Thesis Mentor
Dr. Gonzalo Campillo-Alvarado, Thesis Mentor

Prof. Claudio J Margulis, Chemistry Honors Advisor

Copyright by
Elizabeth A. Keene
2020
All Rights Reserved

Dedicated to Jayne.

ACKNOWLEDGEMENTS

I'd like to thank Dr. Campillo-Alvarado and Professor MacGillivray for their continued support
and guidance.

ABSTRACT

Emtricitabine (trade name: Emtriva) is an anti-HIV prevention and treatment drug. Emtricitabine (EMT) is used along with Tenofovir to form the combination-drug, Truvada, which is extremely effective in the prevention and treatment of HIV. Emtricitabine works by inhibiting reverse transcriptase and is conventionally administered orally in a tablet. Only one solid form corresponding to the pure drug is currently known. Cocrystallization is a method of creating novel solid forms by combining two or more components. In this context, cocrystallization is a good strategy to generate new and enhanced solid forms of Emtricitabine. Through our work with Emtricitabine, we generated new cocrystals with bipyridines using mechanochemical techniques. The new solids were studied and characterized using X-ray diffraction techniques such as powder X-ray diffraction and single crystal X-ray diffraction. We anticipate our work could lead to the design of improved solids of Emtricitabine that could be used in new administration routes of the drug.

INTRODUCTION:

Emtricitabine (EMT) is a nucleoside reverse transcriptase inhibitor that inhibits the viral replication of HIV. It is used in a combination therapy as a treatment for patients with HIV. Emtricitabine is also used in combination with tenofovir as a HIV viral replication preventative drug: Truvada¹. In this combination, EMT is listed in the WHO Model List of Essential Medicines as one of the most important medicines needed to treat the needs of patients globally².

EMT, along with most prescribed drugs, are most commonly administered orally³. In our research, we aimed to find different solid forms of Emtricitabine with improved chemical and physical properties.

In order to do this, we utilized crystal engineering, a field that employs known non-covalent interactions (supramolecular chemistry) and their properties in order to develop new solids. One strategy of crystal engineering is cocrystallization.

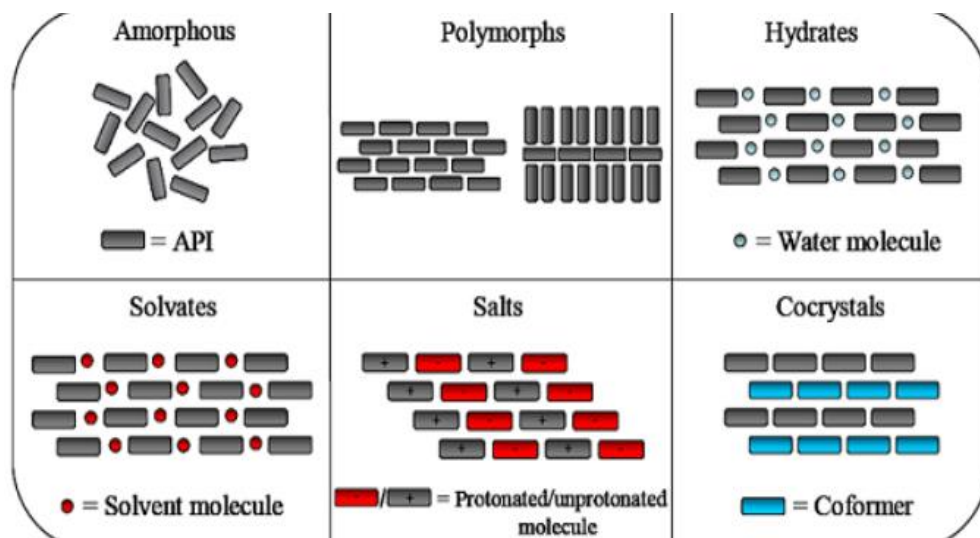


Figure 1. Example of the different strategies to obtain new solid forms of drugs⁴.

Cocrystallization is the process where two or more molecules interact with each other through non-covalent interactions in a crystal lattice. One of the ways to promote

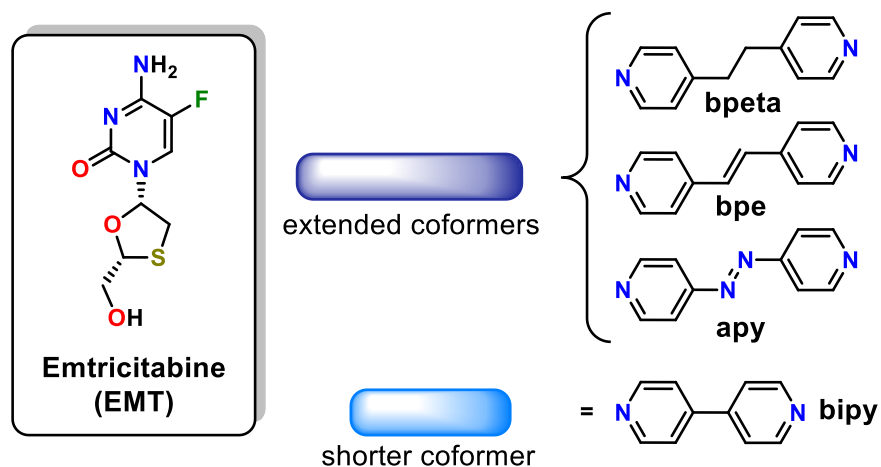
cocrystallization is through mechanochemistry through liquid assisted grinding (LAG).

Mechanochemistry is a technique where solids are ground together, and the mechanical energy promotes reactions between the different molecules⁵. This is a green chemistry technique because a minimal amount of solvent is used.

We used mechanochemistry in order to generate new solid forms of EMT improved chemical and physical properties. These new properties could lower the cost of production and enhance effectiveness. Other possibilities are new routes of administration for the drug: such as topically. Our research involving the cocrystallization of EMT also gives us an idea of how the drug interacts with other solid forms. Since EMT is typically used in combination therapies, this information could be applied in the future to predict interactions and to create solids of the EMT with improved physicochemical properties. This could improve the function of EMT in its role to prevent and treat HIV infection.

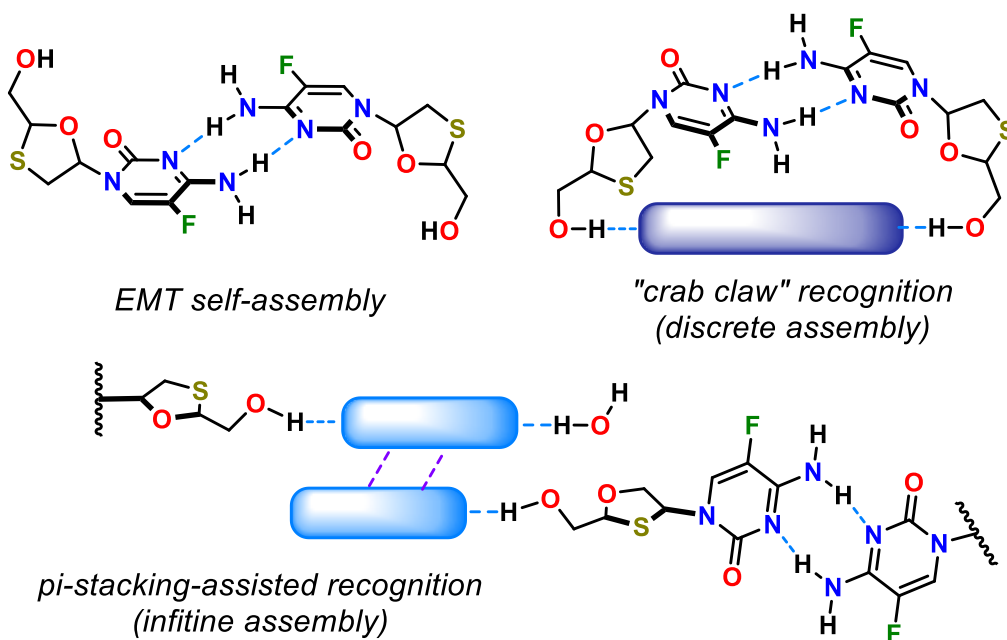
Cocrystallization has been successful in the endeavor of improving a drug's function before. For example, Entresto was the first cocrystal approved by the FDA. Entresto is a drug used in the treatment of heart disease. It is a combination of sacubitril and valsartan⁶.

We report in this thesis, four novel cocrystals of EMT with bipyridines: 4'4-bipyridine (bpy), 1,2- bis(4-pyridyl)ethane (bpeta), 4,4'-azopyridine (apy), and 1,2-bis(4-pyridyl)ethene (bpe) (Scheme 1).



Scheme 1: The molecular structures of EMT and bipyridines.

Specifically, we modulated hydrogen bondings and π - π interactions in order to stabilize and form crystalline structures. The cocrystals self-assembled in either cleft conformation (bpeta, bpe and apy) or in catemer conformation (bpy) (Scheme 2).



Scheme 2: The prior known EMT solid state conformation and the two novel conformations.

EXPERIMENTAL:

Grinding Experiment: All chemicals were used as received from the vendors. EMT was purchased from Combi Blocks, while bpe, bpy, bpeta and apy were purchased from Aldrich.

Cocrystals (EMT)₂·(bpeta), (EMT)₂·(bpe) and (EMT)₂·(apy) were obtained by combining EMT (40 mg, 0.162 mmol) with the corresponding bipyridine (0.081 mmol) through liquid-assisted grinding (LAG, methanol). Cocrystal (EMT)₂·(bpy)₂·H₂O was obtained by combining EMT (40 mg, 0.162 mmol) with 4,4'-bipyridyl (25.3 mg, 0.162 mmol). Once grinding was completed, we took the powder and analyzed it to verify product formation using Powder X-Ray Diffraction.

Powder X-Ray Diffraction (PXRD): The samples were transferred, in powder form, from the mortar-and-pestle to a glass slide for PXRD. PXRD information was collected using a Bruker D-8 ADVANCE X-ray diffractometer with Cu K α radiation ($\lambda = 1.54056 \text{ \AA}$) and a LynxEye detector. Samples were collected from 5° to 35° 2 θ (count time: fast continuous PSD, step size: 0.019°). The machine was operated at 40 kV and 30 mA, and data was acquired at room temperature.

Cocrystal Synthesis: Our samples, still in powdered form, were dissolved in minimal methanol purchased from Aldrich. 2(EMT)·(bpeta), 2(EMT)·(apy), (EMT)·(bpy) and 2(EMT)·(bpe) were each dissolved in separate vials, heated to a boil to ensure complete dissolution and then left to slowly evaporate at room temperature. As the solvent evaporated away the crystals formed. The resulting crystals were analyzed using Single Crystal X-Ray Diffraction.

Single Crystal X-ray Diffraction (SCXRD): Data for 2(EMT)·(bpeta), 2(EMT)·(apy), (EMT)·(bpy) and 2(EMT)·(bpe) was measured on a Bruker D-8 Venture diffractometer equipped with a Duo-Photon 3 area detector using Mo-K α radiation ($\lambda_{\text{MoK}\alpha} = 0.71073 \text{ \AA}$, diffraction source: Incoatec micro-source 3.0 Mo). The frames were integrated with the Bruker SAINT software package using a narrow-frame algorithm. Data were corrected for absorption effects using the Multi-Scan method (SADABS). Structure solution, refinement and data output were carried out with the Olex2 software package. Programs from the Olex2 software package were then used in data reduction. Structure and arrangement solutions were then determined using ShelXL and ShelXT from the Olex2 graphical user interface. Data was then solved and refined using the Olex2 interface. All non-hydrogen atoms were refined using anisotropic displacement parameters. Illustrations of SCXRD data were made using MERCURY. In order to confirm our data the formation of new solids and stoichiometries of single crystals, spectra of the cocrystals were collected using ^1H NMR spectroscopy and IR spectroscopies.

NMR: ^1H NMR data was collected using a Bruker AVANCE 300 NMR spectrometer operating at 300 MHz using DMSO- d_6 as the solvent. Signal assignment for EMT was based on previous reports and all data was processed with Mnova suite⁷.

IR: Data was collected using a Thermo Scientific Nicolet 380 FT-IR spectrometer and measured in the range of 3600-750 cm^{-1} . The FT-IR spectrometer equipped with a diamond ATR crystal.

RESULTS AND DISCUSSION

When we began our research, the only known solid form of EMT was a dimer with itself⁸. Molecules of EMT were bonded together forming a dimer (Figure 2a, b) with hydrogen bonds. The nitrogen atoms acted as donors while the NH and OH groups acted as acceptors (Figure 2c) as depicted below in Figure 2.

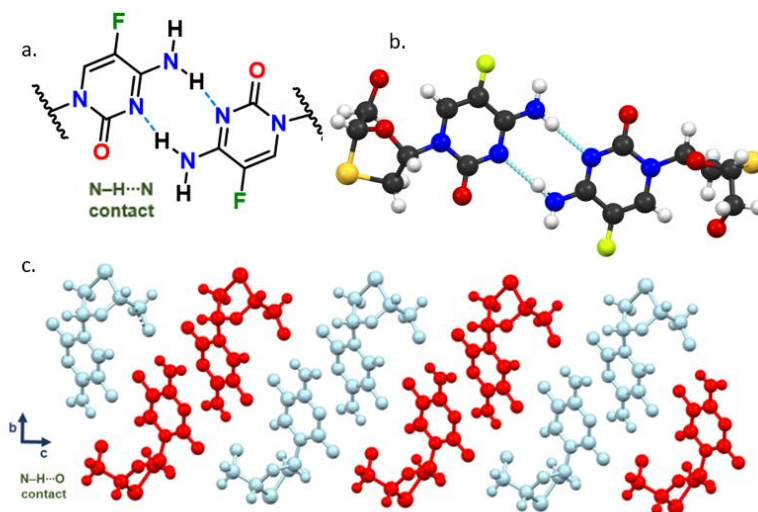


Figure 2: (a) Crystal structure of commercially available EMT, (b) dimer formation, and (c) crystal packing of EMT.

Our experiment involved the combination of bipyridines and EMT. We combined each of the solid bipyridines with solid EMT in a mortar-and-pestle. In order to promote the formation of a new solid phase, we applied mechanochemistry for fifteen minutes using a drop of methanol as a solvent. The resulting solid was then dissolved into methanol, heated and left to evaporate. The results, after two days of slow evaporation, were crystals suitable for SCXRD.

The product resulting from the EMT and bpeta combination, 2(EMT)·(bpeta), self-assembled as discrete assemblies or, as we refer to it, in supramolecular clefts. This means that

the molecular structure resembles purely organic covalent molecular clefts from Rebek's clefts (Figure 3)⁹.

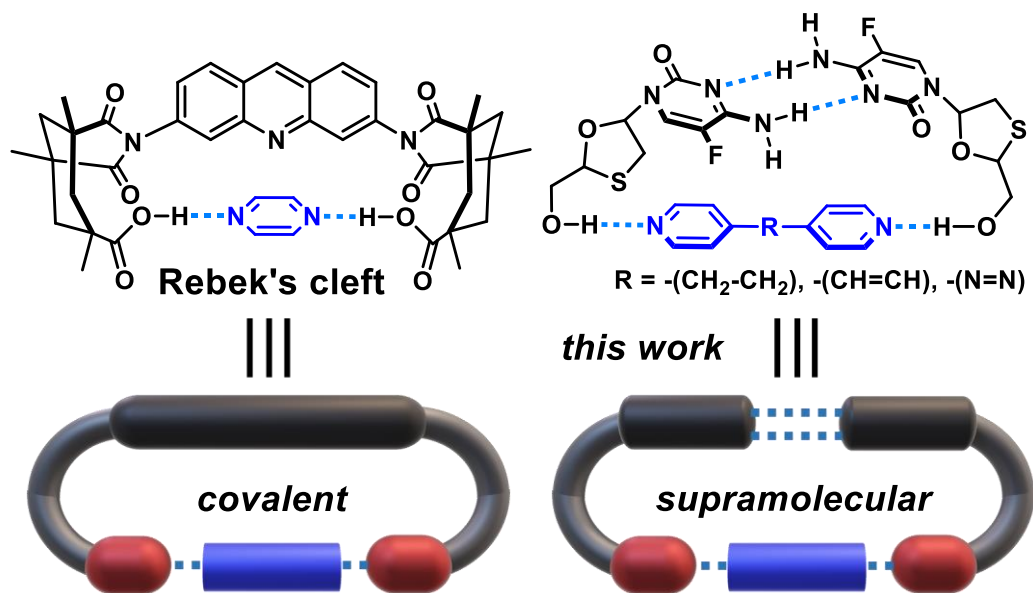


Figure 3: Conformation of the cleft geometry, Rebek's covalent cleft on the left and our novel supramolecular cleft on the right.

In order to create these supramolecular clefts, we first had to utilize liquid assisted grinding in order to promote the formation of a new solid phase. We analyzed the resulting powder using PXRD in order to confirm the formation of a new solid form. In the cocrystal pattern, some starting material peaks are visible in addition to novel peaks which are shown in Figure 4.

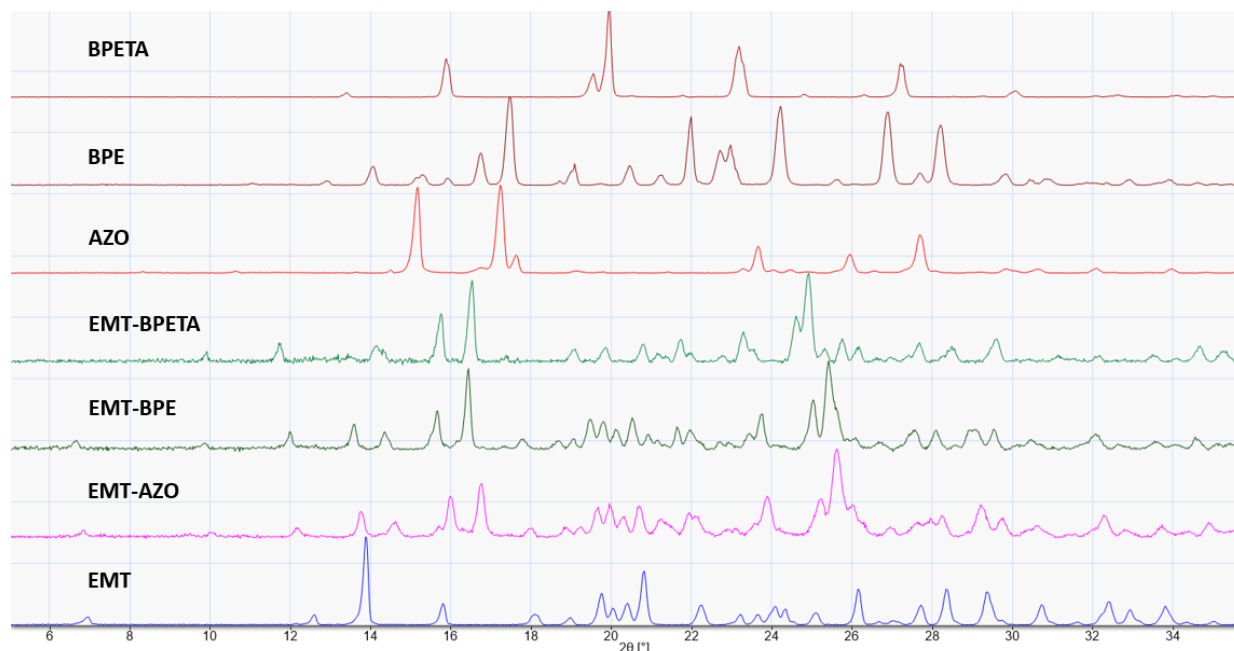


Figure 4: The PXRD patterns of the starting materials and the cocrystals.

The appearance of novel peaks confirmed we had a new solid phase and in order to further analyze the structure, we used to use SCXRD. In order to employ this method, we needed to grow suitable single crystals via slow evaporation of a methanol solution with the powder completely dissolved.

SCXRD revealed that, in order to form our supramolecular cleft, two EMT molecules interact with the bpeta bipyridine through O-H \cdots N hydrogen bonds. The two EMT molecules self-assembled forming a dimer through N-H \cdots N hydrogen bonds. Additional π - π interactions stabilize the supramolecular cleft. Collectively, the result of these interactions is that the two EMT molecules cradle the bipyridine between them. This is illustrated in Figure 5a below. The extended view of the crystal structure in Figure 5b shows a supramolecular sheet in the *bc* plane, composed of the EMT from our cocrystals. The π - π stabilization interactions of the supramolecular columns in the *ac* plane are depicted in Figure 5c.

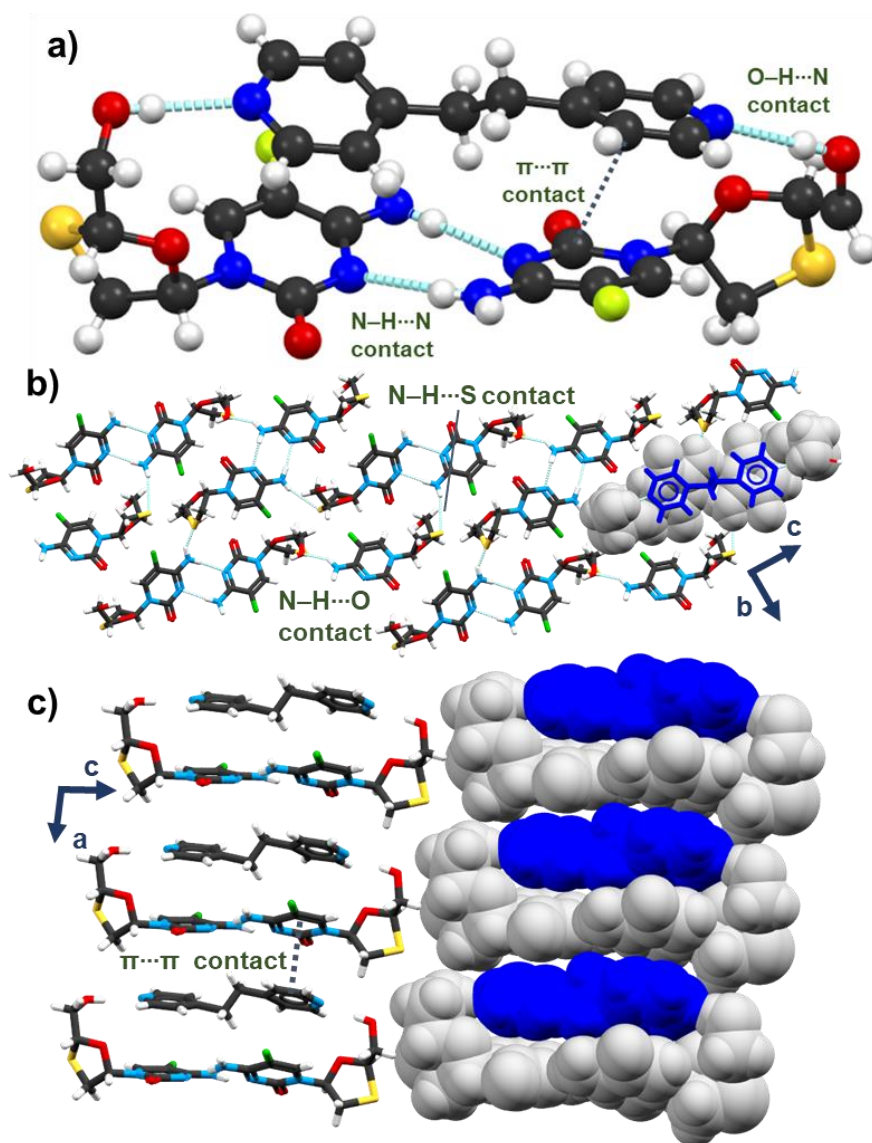


Figure 5: a) The crystal structure of 2(EMT)·bpeta and b) extended packing into layers and c) columns.

The supramolecular cleft defined above is tolerant to multiple bipyridines of similar dimensions. In addition to 2(EMT)·(bpeta): the crystal structure of 2(EMT)·(apy), and 2(EMT)·(bpe) both self-assembled in the same supramolecular cleft conformations, as shown in Figure 6a and 6b below. The cleft similarities are emphasized by an overlay of the cocrystal structures in Figure 6c.

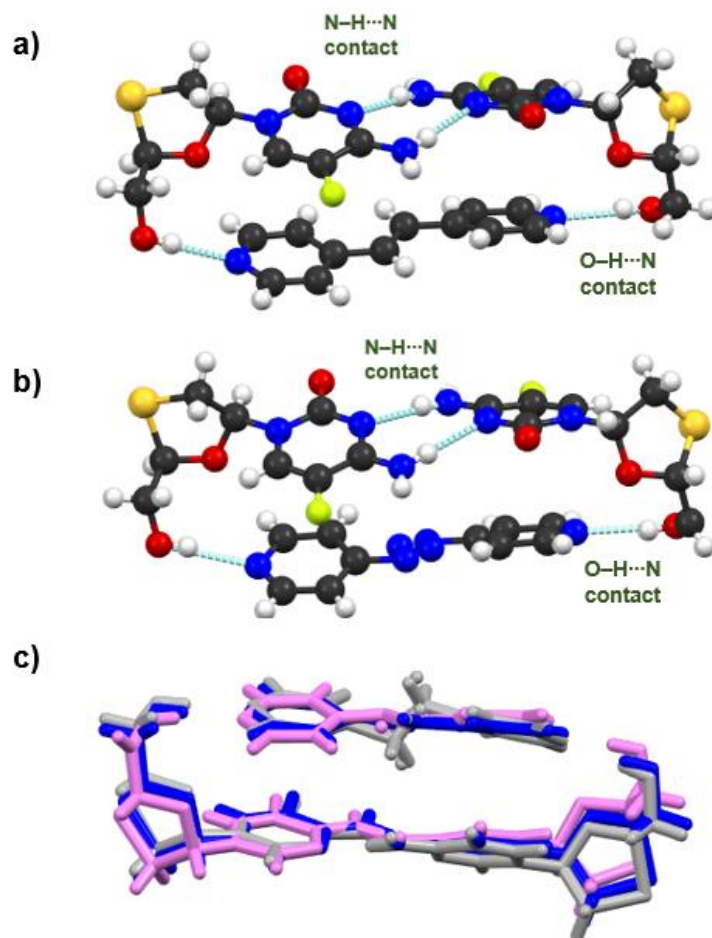


Figure 6: The structures of cocrystals containing bpe and apy and the overlay of the clefts.

A simplistic representation of the crystalline arrangement highlighting the $O-H \cdots N$ bond and the $N \cdots N$ and $O \cdots O$ distances, is shown in Figure 7 below. The bond distances for these interactions are listed in Table 1 below.

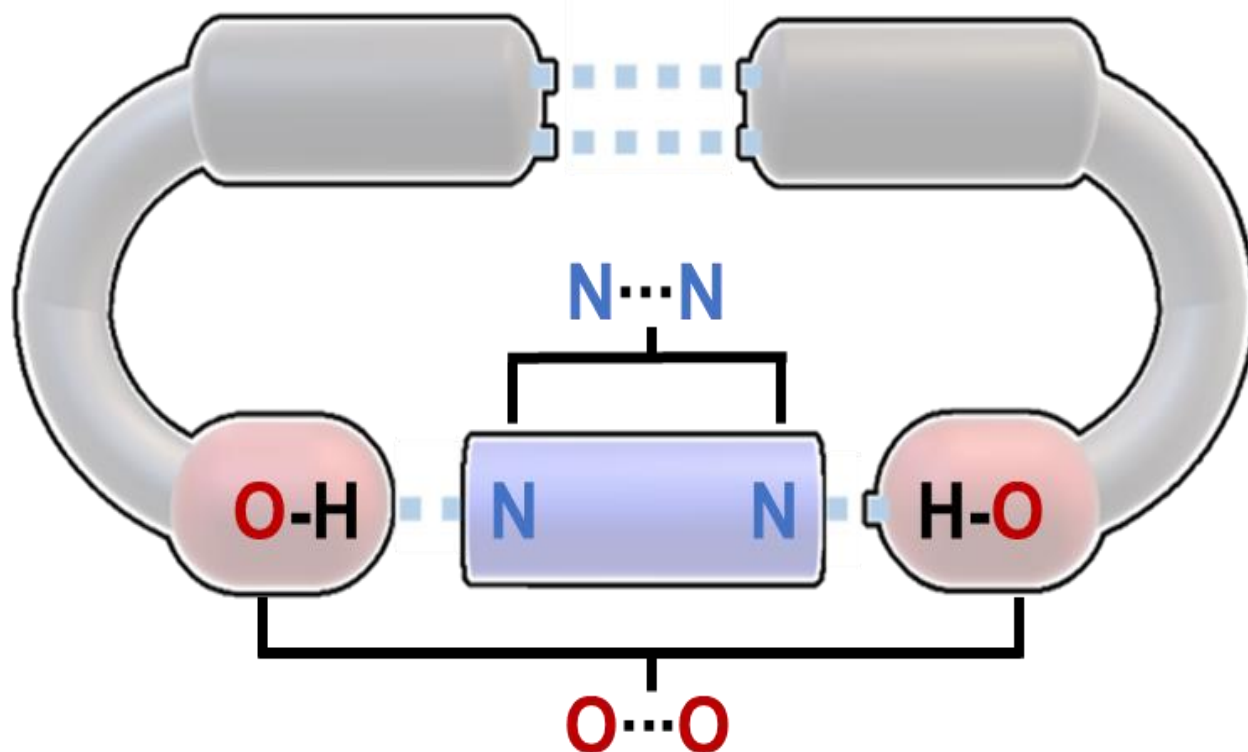


Figure 7: Illustrates the hydrogen bonds and metrics detailed in Table 1 below.

Cocrystal	$d_{\text{O-H}\cdots\text{N}}$ (Å)	$d_{\text{O}\cdots\text{O}}$ (Å)	$d_{\text{N}\cdots\text{N}}$ (Å)
2(FTC)·(b β eta)	2.838(4), 2.850(4)	14.889(4)	9.359(4)
2(FTC)·(b β pe)	2.863(4), 2.858(4)	14.951(4)	9.395(4)
2(FTC)·(a β y)	2.895(5), 2.887(5)	14.676(5)	9.024(5)

Table 1: The hydrogen bond lengths and metrics.

The stoichiometry of the cocrystals was confirmed using ^1H NMR spectroscopy. The spectra obtained from the single crystals provided evidence that the single crystals had two components: EMT and bipyridine. This is depicted below in Figure 8.

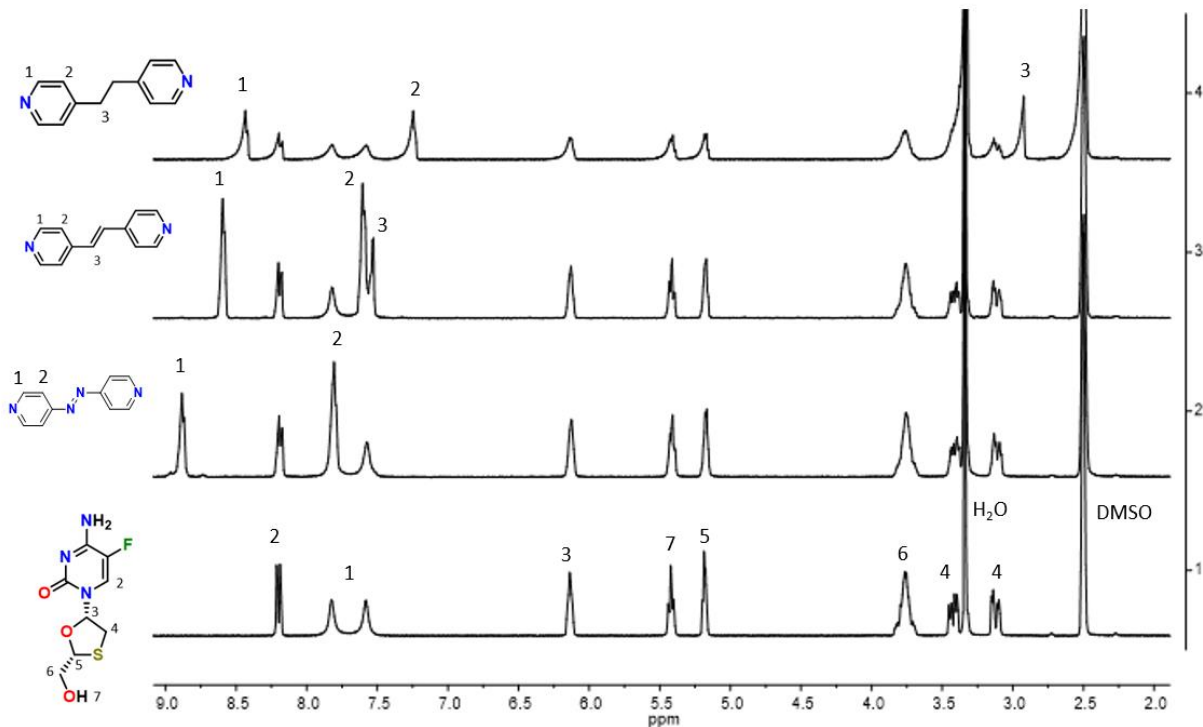


Figure 8: The ¹H NMR spectra of the cocystal products and EMT.

We confirmed the formation of a new solid form through IR spectroscopy using an ATR probe for solids. Formation of cocystal was accompanied by a change in IR bands corresponding to O-H and N-H bonds. This change in signal reaffirmed the formation of novel solid phases. See appendix for spectra.

In order to obtain new solid form with bpy, we employed liquid assisted grinding and analyzed the resulting powder using PXRD. Once again, novel peaks were observed confirming the formation of a new solid phase. These patterns are shown below, in Figure 9.

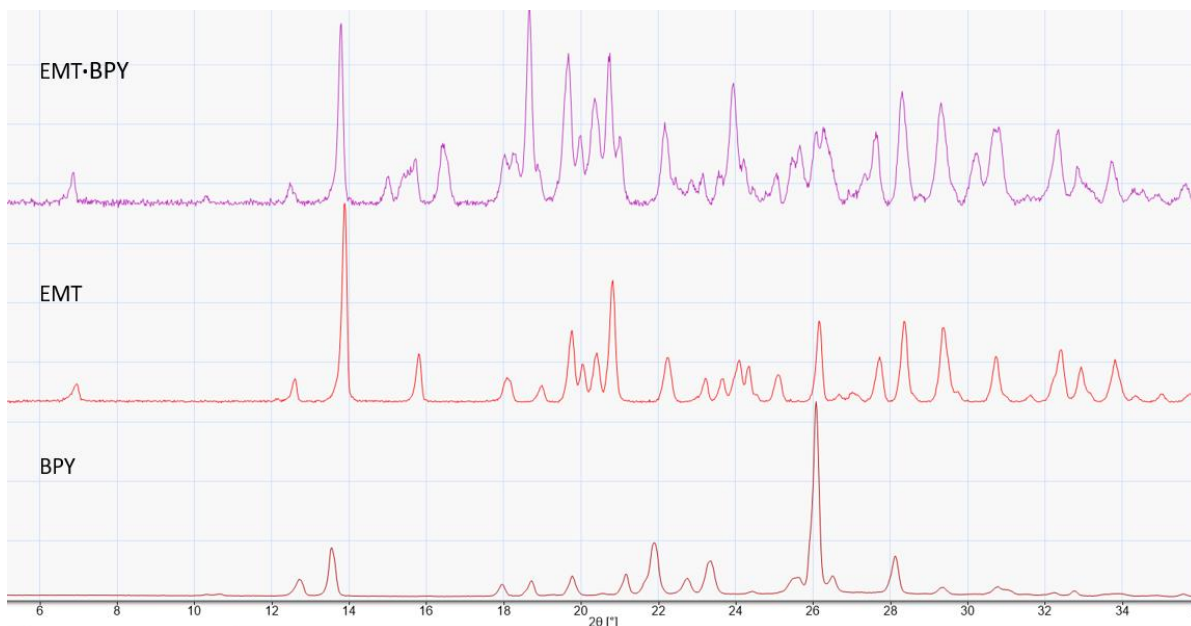


Figure 9: The PXRD pattern of (EMT)·(bpy) cocrystal and starting materials.

While apy, bpeta and bpe all formed similar cocrystal structures in combination with EMT, (EMT)·(bpy), on the other hand, self-assembles into a completely different formation. Bpy has a smaller molecular structure and shorter N···N distances. When this shorter conformer was used, we observed the formation of catemers supported by π - π interactions and hydrogen bonding.

In the catemer structure, as opposed to the cleft where two EMT molecules cradle the bipyridine between them, the molecules form infinite π - π stacks. The EMT molecules in these stacks have a *transoid* conformation. This means the OH groups on the EMT are oriented opposite to each other as opposed to in the *cisoid* conformation observed in the supramolecular cleft.

After confirming the formation of a new solid phase, we employed slow evaporation of methanol to obtain single crystals suitable for use in SCXRD. Crystallographic analysis revealed the components assembled in the infinite stack formation discussed above. In addition to π - π

stacking, a water molecule was identified to support the formation through hydrogen bonds. The cocrystal structure is displayed in Figure 10.

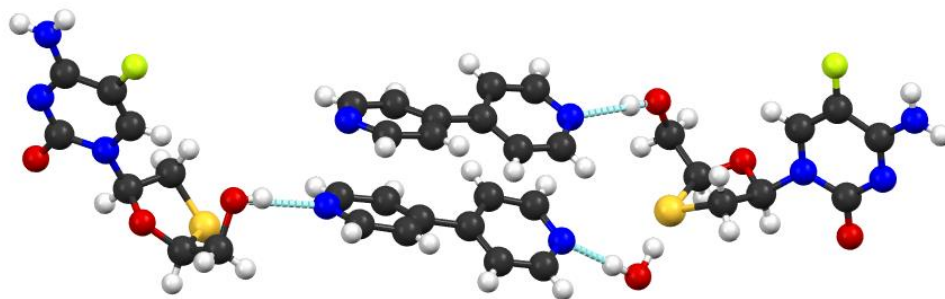


Figure 10: The (EMT)·(bpy) cocrystal structure.

In order to confirm the stoichiometry of the cocrystal, we used ^1H NMR spectroscopy. Additionally, in order to confirm the formation of a new solid phase we utilized IR spectroscopy. The bands of the cocrystal changed intensity and frequency which is in agreement with the formation of a novel solid form.

CONCLUSIONS

Through our research we learned that we can form cocrystals with EMT and various bipyridines. Long bipyridines of the same molecular size will result in formation of similar conformations. In this case our similar sized bipyridines formed a supramolecular cleft. While when a shorter bipyridine was used as a conformer, the assembly of the components shifted to accommodate the change in size and a catemer formation was observed supported by π - π stacking. In the future, we anticipate this research opening doors to create topical administrations of EMT and ultimately the creation of a HIV prevention patch.

REFERENCES

1. Bang, L. M.; Scott, L. J., Emtricitabine. *Drugs* **2003**, *63* (22), 2413-2424.
2. Organization, W. H. *World Health Organization model list of essential medicines: 21st list 2019*; World Health Organization: 2019.
3. Lin, L.; Wong, H., Predicting oral drug absorption: mini review on physiologically-based pharmacokinetic models. *Pharmaceutics* **2017**, *9* (4), 41.
4. Fukte, S. R.; Wagh, M. P.; Rawat, S., Cofomer selection: An important tool in cocrystal formation. *Int J Pharm Pharm Sci* **2014**, *6* (7), 9-14.
5. James, S. L.; Adams, C. J.; Bolm, C.; Braga, D.; Collier, P.; Friščić, T.; Grepioni, F.; Harris, K. D.; Hyett, G.; Jones, W., Mechanochemistry: opportunities for new and cleaner synthesis. *Chemical Society Reviews* **2012**, *41* (1), 413-447.
6. Chavan, R. B.; Thipparaboina, R.; Yadav, B.; Shastri, N. R., Continuous manufacturing of co-crystals: challenges and prospects. *Drug delivery and translational research* **2018**, *8* (6), 1726-1739.
7. Caso, M. F.; D'Alonzo, D.; D'Errico, S.; Palumbo, G.; Guaragna, A., Highly stereoselective synthesis of lamivudine (3TC) and emtricitabine (FTC) by a novel N-glycosidation procedure. *Organic letters* **2015**, *17* (11), 2626-2629.
8. Van Roey, P.; Pangborn, W.; Schinazi, R.; Painter, G.; Liotta, D., Absolute Configuration of the Antiviral Agent (–)-cis-5-Fluoro-1-[2-Hydroxymethyl]-1, 3-Oxathiolan-5-yl] Cytosine. *Antiviral Chemistry and Chemotherapy* **1993**, *4* (6), 369-375.
9. Rebek, J.; Nemeth, D., Molecular recognition: Ionic and aromatic stacking interactions bind complementary functional groups in a molecular cleft. *Journal of the American Chemical Society* **1986**, *108* (18), 5637-5638.

APPENDIX

Crystal Data and Structural Refinement Tables

Table 2: Crystal data and structure refinement for EMT-apy.

Identification code	EMT-apy
Empirical formula	C ₂₆ H ₂₇ F ₂ N ₁₀ O ₆ S ₂
Formula weight	677.69
Temperature/K	296.15
Crystal system	monoclinic
Space group	P2 ₁
a/Å	7.5024(8)
b/Å	11.2194(11)
c/Å	18.2134(18)
α/°	90
β/°	100.538(5)
γ/°	90
Volume/Å ³	1507.2(3)
Z	2
ρ _{calc} /g/cm ³	1.493
μ/mm ⁻¹	0.249
F(000)	702.0
Crystal size/mm ³	0.13 × 0.095 × 0.02
Radiation	MoKα (λ = 0.71073)
2θ range for data collection/°	4.55 to 55.786
Index ranges	-9 ≤ h ≤ 9, -14 ≤ k ≤ 14, -23 ≤ l ≤ 23
Reflections collected	32670
Independent reflections	7064 [R _{int} = 0.0428, R _{sigma} = 0.0350]
Data/restraints/parameters	7064/6/424
Goodness-of-fit on F ²	1.073
Final R indexes [I ≥ 2σ (I)]	R ₁ = 0.0487, wR ₂ = 0.1106
Final R indexes [all data]	R ₁ = 0.0591, wR ₂ = 0.1157
Largest diff. peak/hole / e Å ⁻³	0.48/-0.22
Flack parameter	0.04(2)

Table 3: Crystal data and structure refinement for EMT-bpy.

Identification code	EMT-bpy
Empirical formula	C ₃₆ H ₃₈ F ₂ N ₁₀ O ₇ S ₂
Formula weight	824.895
Temperature/K	150.15
Crystal system	monoclinic
Space group	P2 ₁
a/Å	7.4668(10)
b/Å	9.6700(14)
c/Å	26.187(4)
α/°	90
β/°	90.087(4)
γ/°	90
Volume/Å ³	1890.8(5)
Z	2
ρ _{calc} /cm ³	1.449
μ/mm ⁻¹	0.215
F(000)	860.9
Crystal size/mm ³	0.115 × 0.1 × 0.06
Radiation	Mo Kα (λ = 0.71073)
2θ range for data collection/°	4.5 to 52.98
Index ranges	-9 ≤ h ≤ 9, -12 ≤ k ≤ 12, -32 ≤ l ≤ 32
Reflections collected	48450
Independent reflections	7767 [R _{int} = 0.0550, R _{sigma} = 0.0423]
Data/restraints/parameters	7767/49/508
Goodness-of-fit on F ²	1.038
Final R indexes [I ≥ 2σ (I)]	R ₁ = 0.0559, wR ₂ = 0.1267
Final R indexes [all data]	R ₁ = 0.0633, wR ₂ = 0.1307
Largest diff. peak/hole / e Å ⁻³	0.42/-0.39
Flack parameter	0.3(4)

Table 4: Crystal data and structure refinement for EMT-bpe.

Identification code	EMT-bpe
Empirical formula	C ₂₈ H ₃₀ F ₂ N ₈ O ₆ S ₂
Formula weight	676.72
Temperature/K	298.15
Crystal system	monoclinic
Space group	P2 ₁
a/Å	7.4883(7)
b/Å	11.2957(11)
c/Å	18.1735(18)
α/°	90
β/°	100.406(5)
γ/°	90
Volume/Å ³	1511.9(3)
Z	2
ρ _{calc} /cm ³	1.486
μ/mm ⁻¹	0.246
F(000)	704.0
Crystal size/mm ³	0.145 × 0.065 × 0.03
Radiation	MoKα (λ = 0.71073)
2θ range for data collection/°	5.532 to 56.542
Index ranges	-9 ≤ h ≤ 9, -14 ≤ k ≤ 13, -24 ≤ l ≤ 17
Reflections collected	12872
Independent reflections	6094 [R _{int} = 0.0238, R _{sigma} = 0.0337]
Data/restraints/parameters	6094/1/417
Goodness-of-fit on F ²	1.059
Final R indexes [I ≥ 2σ (I)]	R ₁ = 0.0369, wR ₂ = 0.0838
Final R indexes [all data]	R ₁ = 0.0427, wR ₂ = 0.0869
Largest diff. peak/hole / e Å ⁻³	0.26/-0.19
Flack parameter	0.04(2)

Table 5: Crystal data and structure refinement for EMT-bpe

Identification code	EMT-bpeta
Empirical formula	C ₂₈ H ₃₂ F ₂ N ₈ O ₆ S ₂
Formula weight	678.73
Temperature/K	296.15
Crystal system	monoclinic
Space group	P2 ₁
a/Å	7.6333(8)
b/Å	11.2359(11)
c/Å	18.1058(18)
α/°	90
β/°	99.640(5)
γ/°	90
Volume/Å ³	1531.0(3)
Z	2
ρ _{calc} /g/cm ³	1.472
μ/mm ⁻¹	0.243
F(000)	708.0
Crystal size/mm ³	0.185 × 0.055 × 0.05
Radiation	MoKα (λ = 0.71073)
2θ range for data collection/°	5.512 to 49.994
Index ranges	-9 ≤ h ≤ 9, -13 ≤ k ≤ 13, -21 ≤ l ≤ 21
Reflections collected	15295
Independent reflections	5271 [R _{int} = 0.0313, R _{sigma} = 0.0339]
Data/restraints/parameters	5271/1/446
Goodness-of-fit on F ²	1.024
Final R indexes [I >= 2σ (I)]	R ₁ = 0.0292, wR ₂ = 0.0677
Final R indexes [all data]	R ₁ = 0.0325, wR ₂ = 0.0700
Largest diff. peak/hole / e Å ⁻³	0.14/-0.15
Flack parameter	0.02(3)

NMR Spectra

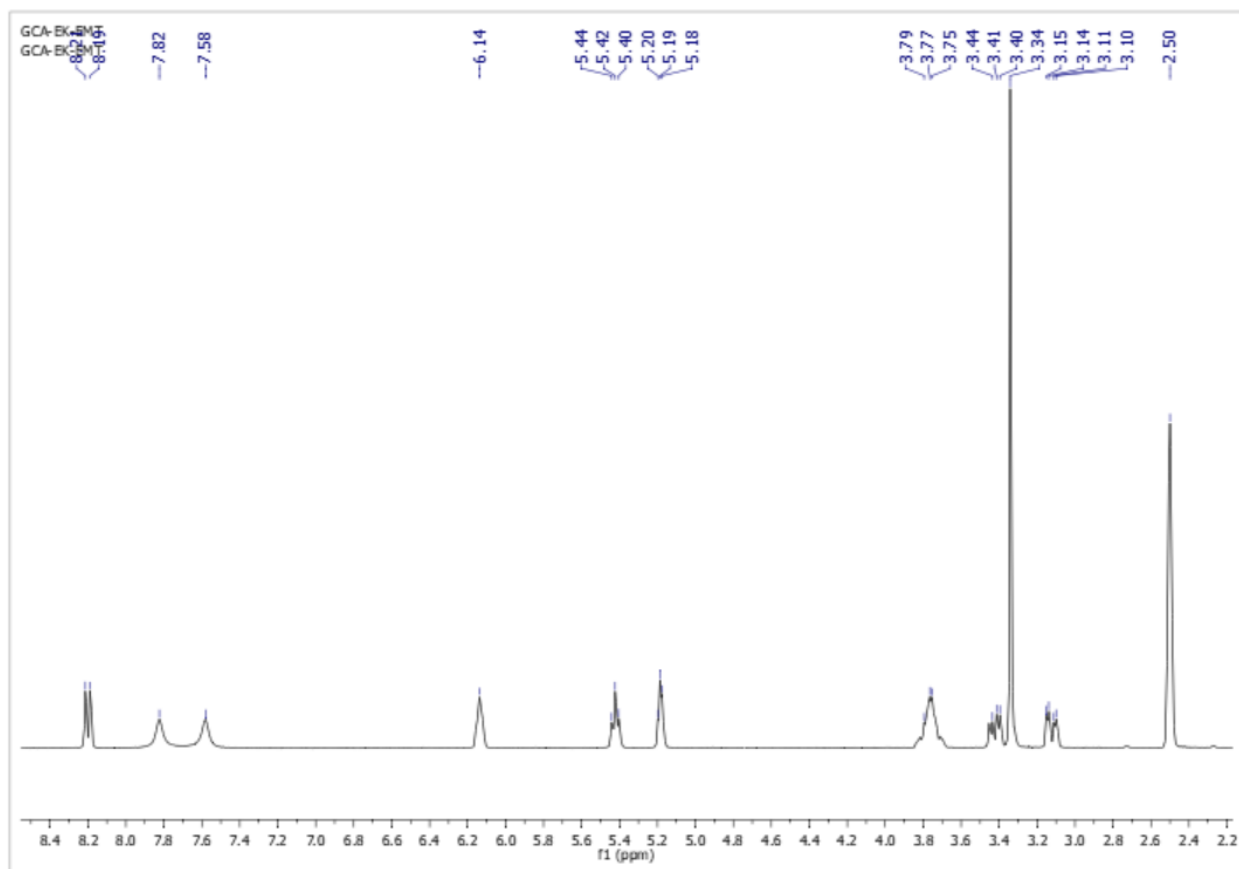


Figure 11: ¹H NMR spectra of EMT (300 MHz, DMSO-d₆)

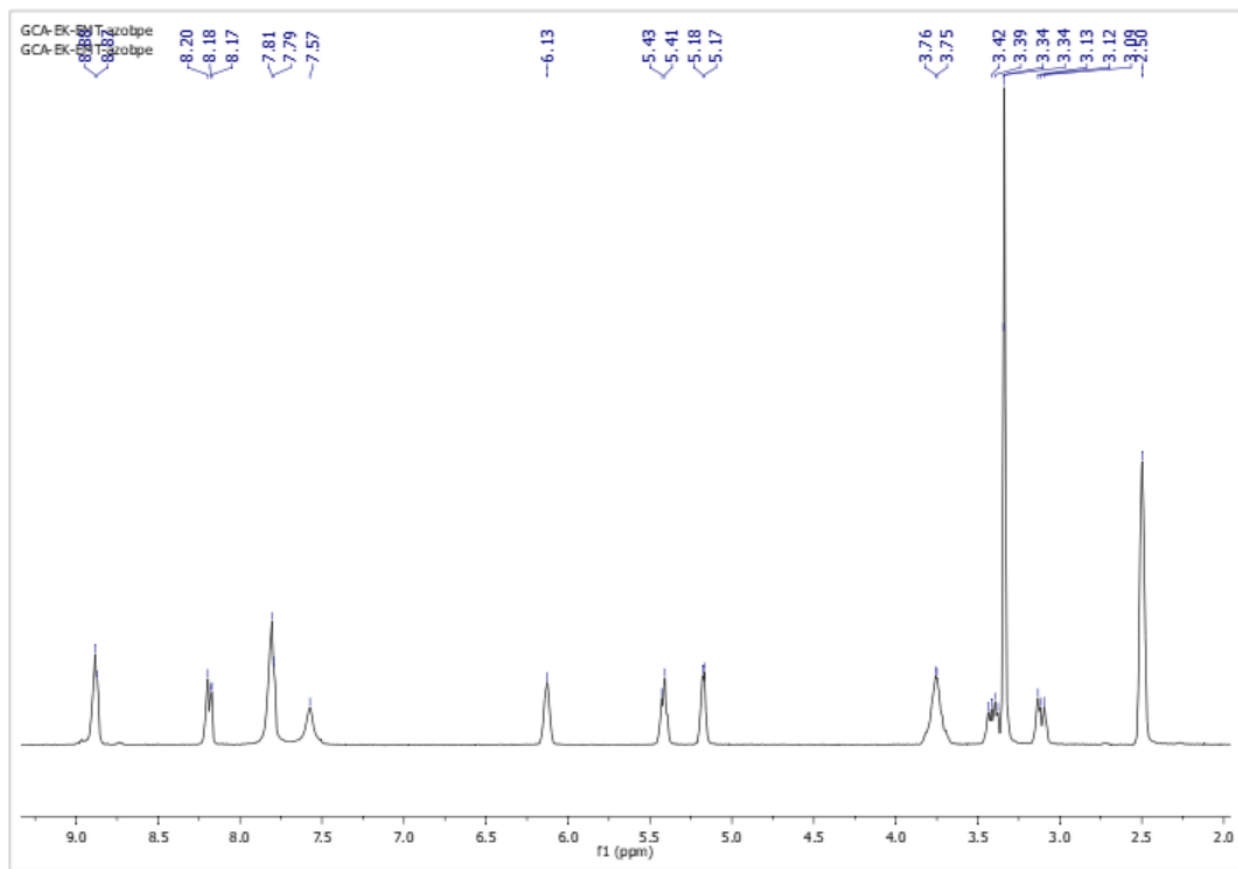


Figure 12: ¹H NMR spectra of EMT-apy (300 MHz, DMSO-d₆)

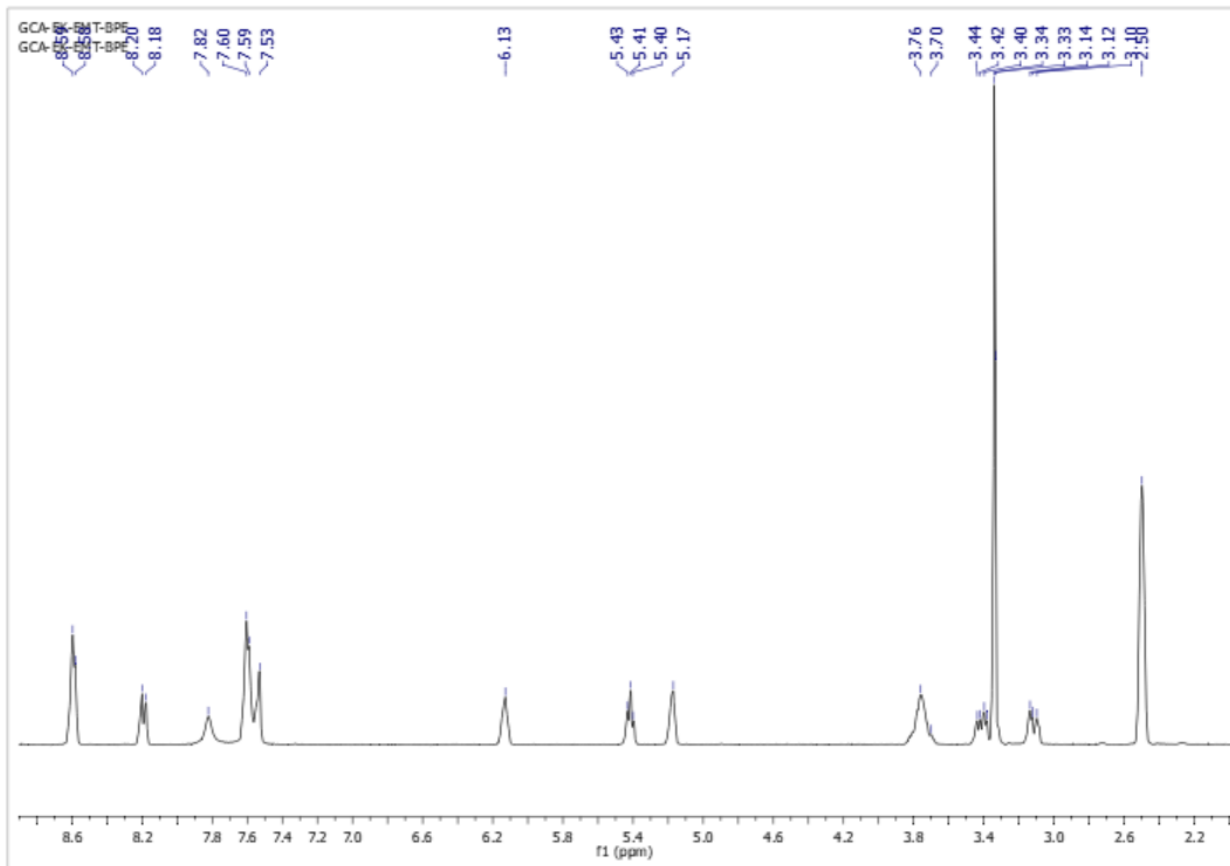


Figure 13: ¹H NMR spectra of EMT-bpe (300 MHz, DMSO-d₆)

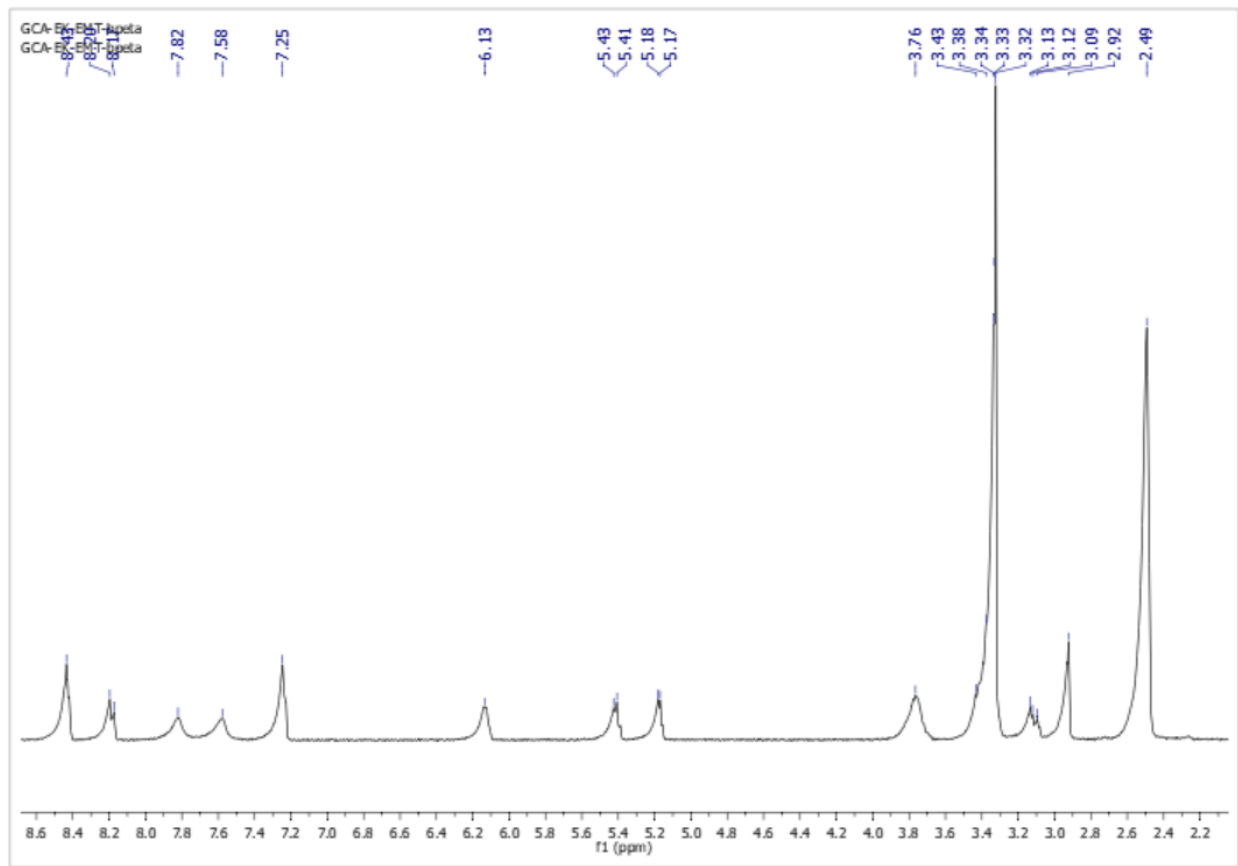


Figure 14: ¹H NMR spectra of EMT-bpeta (300 MHz, DMSO-d₆)

IR Spectra

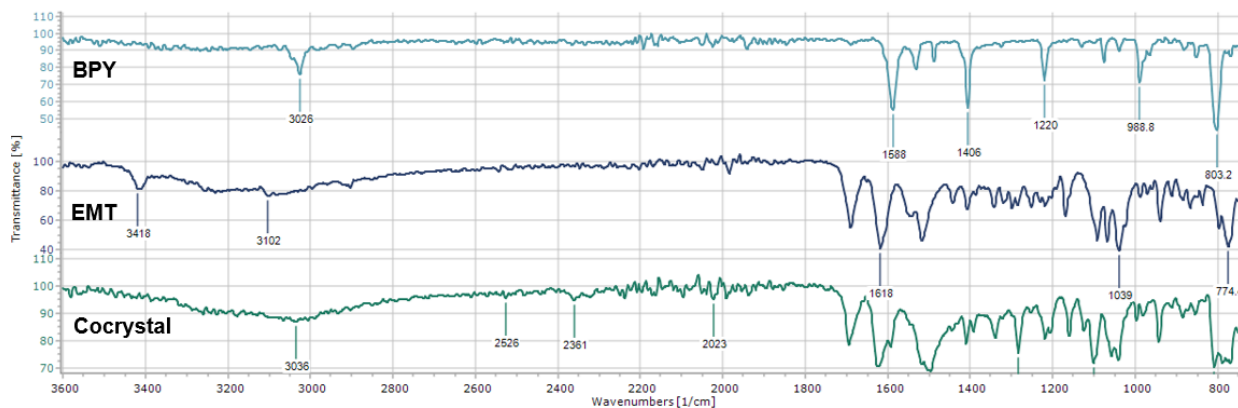


Figure 15: ATR-IR spectrum of (EMT)·(bpy) and starting materials.

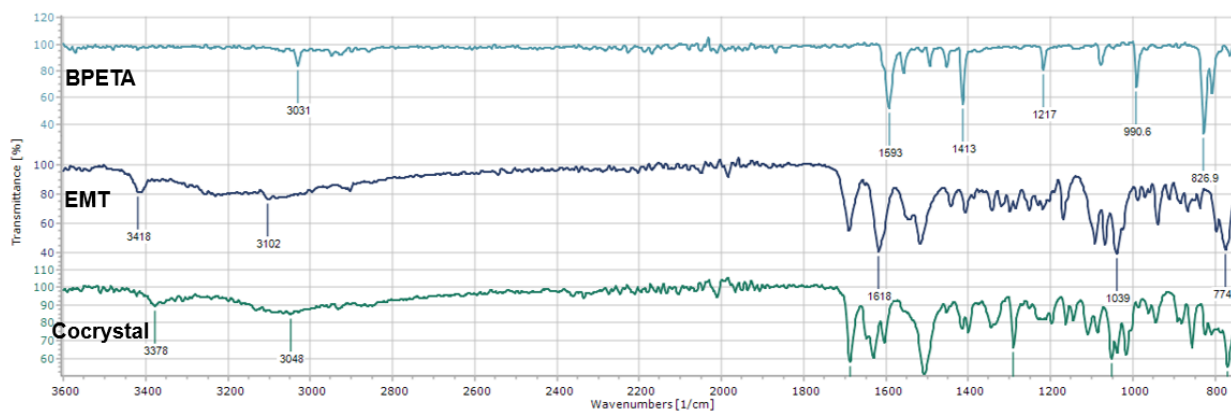


Figure 16: ATR-IR spectrum of (EMT)·(bpeta) and starting materials.

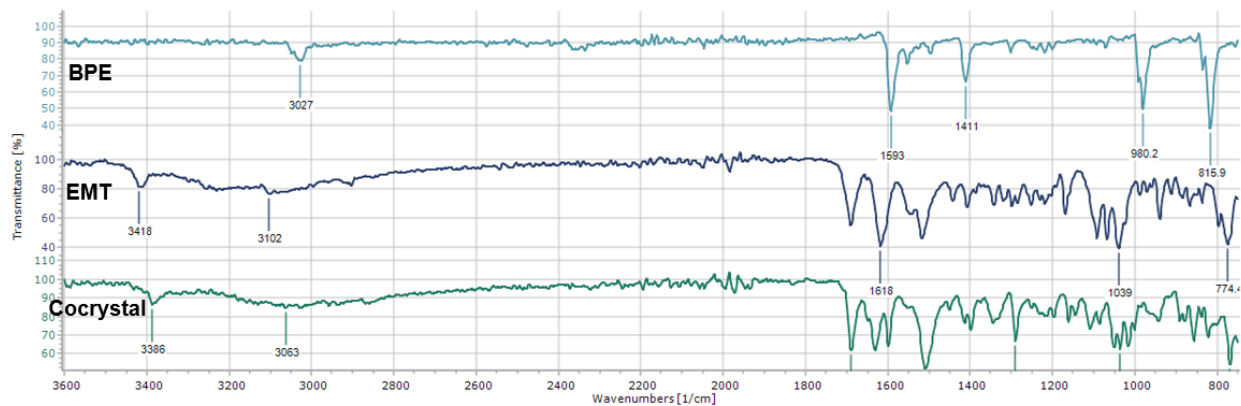


Figure 17: ATR-IR spectrum of (EMT)·(bpe) and starting materials.

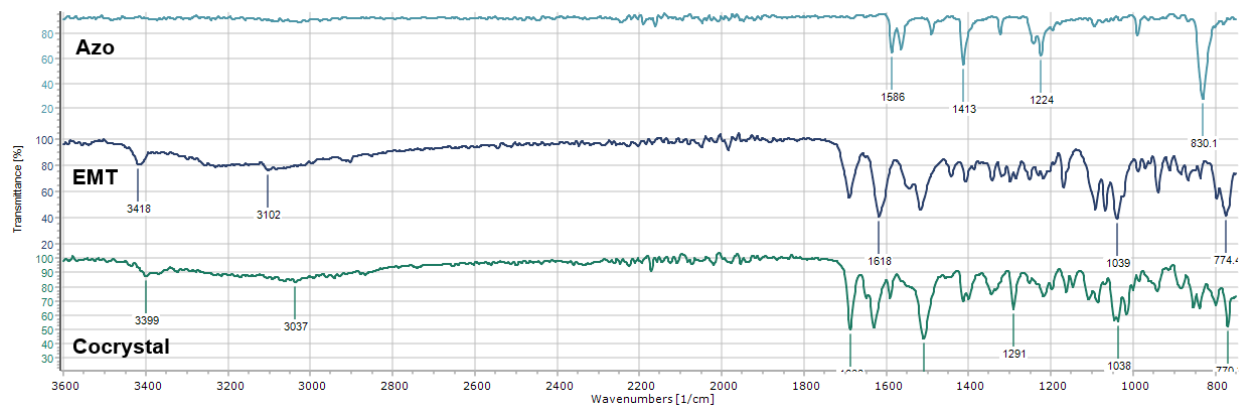


Figure 18: ATR-IR spectrum of (EMT)·(azo) and starting materials.